J. Fluid Mech. (1987), *vol.* 181, *pp.* 519–525
Printed in Great Britain

A note on the generation of Tollmien–Schlichting waves by sudden surface-curvature change

By M. E. GOLDSTEIN AND LENNART S. HULTGREN
National Aeronautics and Space Administration, Lewis Research Center, Cleveland, OH 44135, USA

(Received 14 July 1986)

This note is primarily concerned with the generation of spatially growing Tollmien–Schlichting waves by the interaction of very long-wavelength free-stream disturbances with a discontinuity in the curvature of a bounding surface (whose slope may or may not be continuous). The theory is combined with a numerical solution of the local Orr–Sommerfeld equation, and the result is used to predict the Tollmien–Schlichting amplitude in a relevant experiment carried out by Leehey & Shapiro (1980). The calculated results are in satisfactory agreement with their observations.

1. Introduction

Goldstein (1985, hereinafter referred to as I) showed that small but sudden changes in surface geometry can produce strong coupling between long (effectively infinite)-wavelength free-stream disturbances and very short-wavelength boundary-layer instability waves. The analysis was compared with the Leehey & Shapiro (1980) receptivity experiment and was found to provide a possible explanation for the very large (i.e. order-one) coupling coefficient that was observed there. The comparison was, for simplicity, carried out by calibrating an existing calculation of the steady flow over a wall with a sudden slope change with Shapiro's (1977) static pressure measurements. But the experimental geometry had only surface-curvature discontinuity with no discontinuity in wall slope.

This note extends the calculation of I to these higher-order discontinuities and shows that the result can still predict the order-one coupling coefficient observed by Leehey & Shapiro (1980). The comparison now proceeds directly from the prescribed surface geometry without artificial calibration with the measured pressure, which we feel is important because it demonstrates how an apparently smooth surface can serve as an initiation site for Tollmien–Schlichting waves. We also give an improved estimate of the instability-wave amplification between the source region and measuring station. This is done by solving an Orr–Sommerfeld equation with numerically calculated mean-velocity profiles.

2. Analysis

As in I, we begin by considering the steady unseparated flow over a relatively thin, two-dimensional body in an otherwise uniform stream of density ρ_0 and velocity U_∞. We suppose that there is a small region of rapid geometry change located a distance l, say, downstream from the leading edge, which we refer to as the interaction region. The Reynolds number $R = U_{e0}^* l/\nu$, where U_{e0}^* is the velocity at the edge of the

boundary layer at the interaction region and ν is the kinematic viscosity, is assumed to be large, and we require that the ratio l_c/l, where l_c is the distance to the lower branch of the neutral stability curve, remain $O(1)$ as $R \to +\infty$. The length, time, velocity and pressure scales are taken to be l, l/U_{e0}^*, U_{e0}^* and $\rho_0 U_{e0}^{*2}$, respectively.

We again suppose that the interaction-region wall geometry varies on the streamwise lengthscale of a Tollmien–Schlichting wave, which turns out to be $O(\epsilon^3 l)$ where

$$\epsilon = R^{-\frac{1}{8}}. \tag{2.1}$$

The steady flow then exhibits the usual triple-deck structure in this region (Stewartson 1969; Messiter 1970) (see figure 3 of I), and the wall geometry can be described by an equation of the form

$$Y = hF(X), \tag{2.2}$$

where

$$X = x/\epsilon^3, \tag{2.3}$$

$$Y = y/\epsilon^5. \tag{2.4}$$

x and y denote the local non-dimensional streamwise and transverse coordinates at the position of the interacting region; F is an $O(1)$ function of the indicated argument; and h is a real constant.

We suppose that

$$F \to 0 \quad \text{as } X \to +\infty \tag{2.5}$$

and

$$F \sim \alpha_0(-X)^r \quad (r \geqslant 1) \quad \text{as } X \to -\infty, \tag{2.6}$$

where α_0 is an $O(1)$ constant. This local geometry matches onto an outer body-scale geometry that behaves like

$$y \sim \epsilon^{5-3r} h \alpha_0 (-x)^r \quad \text{as } x \to 0-, \tag{2.7}$$

which shows that the body has a thickness ratio σ of $O(\epsilon^{5-3r}h)$. It will exhibit a sudden change in wall slope if $r = 1$; and a sudden change in surface curvature, but no change in wall slope, if $r > 1$. Since the flow cannot remain attached for values of $\epsilon^{5-3r}h$ exceeding $O(1)$, h can only be $O(1)$ if $1 < r < \frac{5}{3}$. Otherwise we must require

$$h = O(\epsilon^{3r-5}). \tag{2.8}$$

The $r = 1$ case, corresponding to a sudden change in wall slope, was analysed by Stewartson (1970) and was the one considered in I. However, Stewartson's (1970) steady-flow triple-deck analysis, and, consequently, the linearized unsteady-flow analysis of I, remain valid for the more general case considered herein. The general theory in Stewartson (1970) is nonlinear (though the actual analysis was only carried for the linear case) and can predict flow reversal (i.e. separation) when h is $O(1)$. It would be interesting to analyse the steady flow with r in the range $1 < r < \frac{5}{3}$ to see if separation is also predicted in this case, but this will not be attempted here.

Stewartson (1970) only worked out the solution for the linear case where $h \ll 1$, which, however, is the only one that is appropriate for the relatively smooth wall with $r > \frac{5}{3}$. This makes the steady flow somewhat uninteresting, but, as we shall see below, the unsteady flow becomes even more interesting.

The Leehey & Shapiro (1980) flat plate consisted of a 6:1 semi-ellipse transitioning

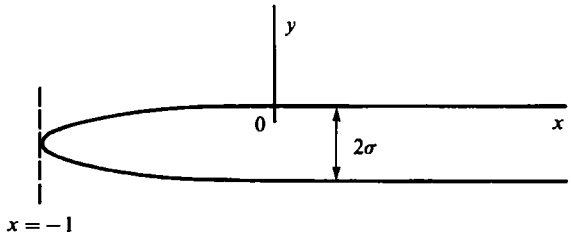

FIGURE 1. Prescribed body geometry.

rather abruptly into the flat-plate section as shown in figure 1. The transverse coordinate y_s of its upper surface is given by

$$y_s = \begin{cases} \sigma((1-x^2)^{\frac{1}{2}}-1) & \text{for } -1 \leqslant x \leqslant 0, \\ 0 & \text{for } x > 0, \end{cases} \tag{2.9}$$

where $\sigma(=\frac{1}{6})$ is the thickness ratio of the semi-ellipse. The function F and the constant h in (2.2) can therefore be taken as

$$F = \begin{cases} -\frac{1}{2}X^2 & \text{for } X < 0, \\ 0 & \text{for } X > 0, \end{cases} \tag{2.10}$$

and

$$h = \epsilon\sigma, \tag{2.11}$$

respectively.

The Tollmien–Schlichting wave generated by the interaction of a small-amplitude free-stream velocity fluctuation with this geometry is still given by (4.9) of I, modified as described in §5.1 of I, i.e. by

$$u_{\mathrm{TS}} = \lambda h \bar{F} A\left(\frac{S_0}{\lambda^{\frac{3}{2}}}\right) U'\left(\frac{y}{\epsilon^4}\right) \exp\frac{\mathrm{i}}{\epsilon^3}\left[\int_0^x \kappa(x)\,\mathrm{d}x - St\right], \tag{2.12}$$

where u_{TS} is the streamwise component of the Tollmien–Schlichting wave velocity normalized by the inviscid streamwise velocity fluctuation just outside the boundary layer at the interaction region, λ is the wall-shear stress just upstream of the interaction region, $S_0 = \epsilon^2 S$, S is the Strouhal number defined in I, A is given by (4.7) in I, U is the local mean-velocity profile, and $\bar{F}(\kappa)$, the Fourier transform of the wall shape function, is now given by

$$\bar{F} = \frac{1}{(2\pi)^{\frac{1}{2}}\mathrm{i}\kappa^3}, \tag{2.13}$$

rather than by (5.1) of I and is still to be evaluated at $x = 0$. The quantity $\lambda h \bar{F} A$ is commonly referred to as the 'coupling coefficient'. Equation (2.11) shows that it is $O(\epsilon\sigma)$, in a formal asymptotic sense. This makes the coupling coefficient of smaller asymptotic order than it was in I, but the viscous parameter ϵ cannot, in reality, be very small if the boundary layer is to remain laminar, and it turns out that the smaller order is actually compensated for by numerically larger values of F.

3. Numerical results

The flat plate in the Leehey & Shapiro (1980) experiment was presumably at zero angle of attack and had a total length L of 168 cm. Also, $l = 3.81$ cm, $U_\infty = 29$ m s^{-1}, and the frequency parameter $\omega\nu/U_\infty^2$ (where ω is the angular frequency) was equal

to 5.6×10^{-5}. (Note that, in addition to the decimal point being misplaced in the text, an incorrect value of 2.1 cm was used for l in (5) of I.)

The inviscid upper-surface velocity was calculated for us by Dr Eric McFarland (of the Lewis Research Center) using his panel-method code. He was limited to an L/l of about 11, for reasons of accuracy, while the experimental value was about 44. However, the shorter plate length probably had little effect on the calculated result in the streamwise region of interest here, since it was found to agree fairly well with a composite thin-airfoil solution for a semi-infinite plate. The panel-method calculation showed that $U_{e0}^*/U_\infty = 1.087$. This value, the previously given numerical values, and an assumed value of $\nu = 15 \times 10^{-6}$ m^2 s^{-1} gives $\epsilon = 0.244$ and $S_0 = 0.226$.

The laminar boundary-layer flow was determined from a finite-difference scheme. Transformed variables, analogous to those described in Schlichting (1979, p. 188), were used, and the governing equations are his (9.64–9.66) with his $N \equiv 1$. They were discretized with central-difference and two-step-backward approximations for derivatives in the normal and streamwise directions, respectively, and the trapezoidal rule was used for the integral. The resulting finite-difference approximation was then solved by iteration at each streamwise station. Each iteration required the solution of a tridiagonal matrix equation and the evaluation of one integral.

The numerical mean-flow calculation suggests that $\lambda = 0.122$, which is about a third of the Blasius boundary-layer value of 0.332. Solving (4.5) of I (which is to be evaluated at $x = 0$) and using (4.4) of I, we find that $|\kappa|$ is approximately equal to 0.140, while figure 5 of I shows that $|A| \approx 1.13$. The coupling coefficient is therefore

$$|\lambda h \bar{F} A| \approx 0.814 \tag{3.1}$$

in this experiment, which is only about one-fourth of the estimate given in I. But we shall now show that the adverse pressure gradient produced a net growth of the instability wave between the interaction region and the measuring station, rather than a net decay as assumed in I.

We used the numerically computed mean-velocity profiles in the Orr–Sommerfeld equation, which was solved numerically at each streamwise location by using the compound-matrix method described in Drazin & Reid (1981). The integration was started in the free stream by using the appropriate asymptotic solutions, and integrated towards the wall using a fourth-order, Adam–Bashforth predictor–corrector method. The procedure was iterated by varying the wavenumber until the wall boundary condition was satisfied to a preset tolerance. The final wavenumber is the desired eigenvalue.

Since the coupling coefficient was determined from a triple-deck analysis, the reader might feel that a triple-deck analysis, such as that of Smith (1979), should also be used to solve the Orr–Sommerfeld problem. But the wavenumber expansion would then have to be carried to fourth order just to determine the instability-wave amplitude to first order, while the coupling coefficient is determined to the same order of accuracy by its lowest-order term. It therefore turns out to be much easier to solve the Orr–Sommerfeld equation numerically. While the asymptotic approach might be more appealing from a pedagogical point of view, it is no more valid than the present scheme, since the formal asymptotic orders of these two approaches are exactly the same.

The imaginary part of the eigenvalue was integrated to yield the growth/damping factor shown in figure 2. The corresponding result for a Blasius boundary layer is also shown. The arrow indicates the location, $x = 3.5$, of the Blasius lower-branch neutral curve. It corresponds to a (Blasius) displacement-thickness Reynolds number

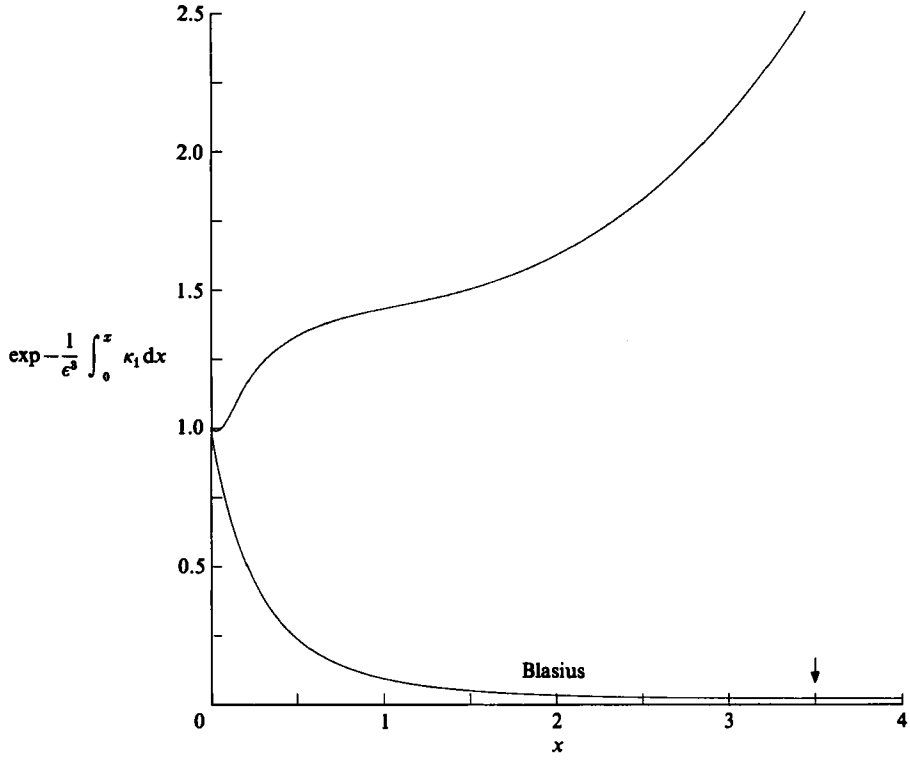

FIGURE 2. Tollmien–Schlichting growth/decay factor.

$Re_\delta = 1.721(xR)^{\frac{1}{2}} \approx 991$. By comparison, $Re_\delta = 467$ at the interaction region. It follows from these results and (2.12) and (3.1) that

$$|u_{TS}|_{max} \approx 2.09\,|U'|_{max} \approx 0.65 \tag{3.2}$$

at the position corresponding to the Blasius lower branch, where the numerical value for $|U'|_{max} \approx 0.309$ incorporates the fact that the interaction-region free-stream velocity, and consequently the acoustic forcing, is 1.087 times the incident value. Equation (3.2) indicates that *the maximum streamwise velocity fluctuation of the Tollmien–Schlichting wave at the position of the Blasius boundary-layer lower branch is approximately two-thirds of the free-stream velocity fluctuation.* It is worth noting that the latter was always less than 3 mm s^{-1} in Shapiro's (1977) experiment.

4. Comparison with the Leehey–Shapiro measurements

Shapiro (1977) measured the total velocity fluctuation in the boundary layer which, as pointed out by Thomas & Lekoudis (1978), probably consisted of the sum of a Stokes shear wave, say $A_S(y)\cos\omega t$, and a Tollmien–Schlichting wave, $A_T(y)\cos(kx-\omega t+\phi)$. A_S is relatively independent of the streamwise coordinate, and the slow streamwise growth or decay of the Tollmien–Schlichting wave is incorporated in A_T. The measured r.m.s. velocity fluctuation amplitude should therefore be of the form

$$A(y) = \tfrac{1}{2}[A_S^2 + A_T^2 + 2A_S A_T \cos(kx+\phi)]^{\frac{1}{2}}. \tag{4.1}$$

As pointed out by Thomas & Lekoudis (1978), figure 28 in Shapiro (1977) (figure 5 in Leehey & Shapiro 1980), which is a plot of

$$\ln\frac{A}{A_0} \equiv \tfrac{1}{2}\ln[1+2b\cos(kx+\phi)+b^2], \tag{4.2}$$

where $b = b(y) = A_T/A_S$, clearly shows the streamwise oscillation of the Tollmien–Schlichting wavenumber predicted by (4.2).

Since the Tollmien–Schlichting wave ultimately exhibits downstream growth (see figure 2), there must be a streamwise location where $|b| = 1$ for each transverse measuring station. The argument of the logarithm can then go to zero in (4.2), causing $\ln A/A_0$ to become infinite. Shapiro's (1977) figure 28 shows a large negative peak at $Re_\delta \approx 990$ – indicating that the Tollmien–Schlichting wave and the Stokes shear wave are of equal magnitude but 180° out of phase at that streamwise location and elevation. The former fortuitously coincides with the lower-branch position for the Blasius boundary layer, as calculated by us† ($Re_\delta = 991$). The Stokes shear wave takes on its free-stream value at the peak Tollmien–Schlichting wave amplitude (which occurs at about one momentum thickness from the wall). *The prediction of* (3.2), *therefore, seems to be about* 33 % *lower than the observed value.*

There are, however, at least two neglected effects that might improve the comparison. First, Shapiro's (1977) figure 28 shows that every second negative peak is clipped – indicating that a second, slowly decaying mode with twice the wavelength may be present in his experiment and that the two modes are in phase at $Re_\delta = 990$. The peak amplitude of the primary mode must therefore be less than unity but probably not as low as two-thirds.

Secondly, our numerical stability calculation does not account for weakly non-parallel mean-flow effects. The latter will always increase the instability-wave growth rate both in the vicinity of and everywhere upstream of the lower branch of the neutral stability curve (Saric & Nayfeh 1977; Smith 1979). These effects could be fairly significant at the relatively low Reynolds numbers involved here, and furthermore, Saric & Nayfeh's (1977) results suggest that they will be more pronounced in the presence of adverse pressure gradients.

The authors would like to thank Dr Eric McFarland for using his panel-method code to calculate the potential flow about Shapiro's plate, and Dr S. J. Cowley for his helpful comments.

REFERENCES

DRAZIN, P. G. & REID, W. H. 1981 *Hydrodynamic Stability*. Cambridge University Press.

GOLDSTEIN, M. E. 1985 Scattering of acoustic waves into Tollmien–Schlichting waves by small streamwise variations in surface geometry. *J. Fluid Mech.* **154**, 509–529.

LEEHEY, P. & SHAPIRO, P. J. 1980 Leading edge effect in laminar boundary layer excitation by sound. In *Laminar–Turbulent Transition* (ed. R. Eppler & H. Fasel), pp. 321–331. Springer.

MESSITER, A. F. 1970 Boundary-layer flow near the trailing edge of a flat plate. *SIAM J. Appl. Maths* **18**, 241–257.

SARIC, W. S. & NAYFEH, A. H. 1977 Nonparallel stability of boundary layers with pressure gradients and suction. In *Laminar–Turbulent Transition, AGARD-CP*-224, pp. 6:1–21.

SCHLICHTING, H. 1979 *Boundary-Layer Theory* (7th edn). McGraw-Hill.

† The theoretical location of the lower branch in Shapiro (1977) is stated to be $Re_\delta = 950$ but is depicted in the range 930–990, depending on which figure one is looking at!

SHAPIRO, P. J. 1977 The influence of sound upon laminar boundary layer instability. *MIT Acoustics and Vibration Lab. Rep.* 83458-83560-1.

SMITH, F. T. 1979 Boundary layers for nonlinear stability of disturbances of various sizes. *Proc. R. Soc. Lond.* A **366**, 91–109.

STEWARTSON, K. 1969 On the flow near the trailing edge of a flat plate. II. *Mathematika* **16**, 106–121.

STEWARTSON, K. 1970 On laminar boundary layers near corners. *Q. J. Mech. Appl. Maths* **23**, 137–152.

THOMAS, A. S. W. & LEKOUDIS, S. G. 1978 Sound and Tollmien–Schlichting waves in a Blasius boundary layer. *Phys. Fluids* **21**, 2112–2113.